Applied Thermal Engineering 278 (2025) 126927

Contents lists available at ScienceDirect

Applied Thermal Engineering

journal homepage: www.elsevier.com/locate/ate

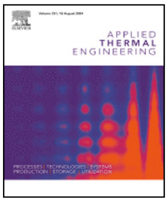

Research Paper

Online characterization of the dynamical state of industrial combustion systems

E. Giulietti [a], E. Giacomazzi [a],[*], C. Stringola [a], C. Romano [b]

[a] TERIN-DEC-CCT Laboratory, ENEA, Rome, Italy
[b] Baker-Hughes, Florence, Italy

ARTICLE INFO

Keywords:
Combustion
Online monitoring
Instability precursor identification
Linear analysis
Industrial burners

ABSTRACT

Although investigated for many years, real-time monitoring of combustion dynamics is still an important issue in modern gas turbine operation. In this article, attention is focused on two quantities, radiant energy and pressure, sampled in an industrial combustion system. Based on such quantities, and with the aim of selecting the best operational index to detect instability precursors, different strategies are here defined and compared. Upon the obtained results, the adopted monitoring and signal analysis strategy reveals promising as an online practical method to detect combustion instabilities.

1. Introduction

Great effort is currently dedicated to the development of fuel-flexible lean-premixed gas turbines able to burn fuel mixtures with variable hydrogen content. Lean premixed combustion offers the advantage of low NO_x emission, but it is highly sensitive to external perturbations, especially to variations in the equivalence ratio of the mixture; this issue tends to promote the onset of self-sustained large amplitude pressure oscillations called thermoacoustic instabilities, due to the resonant coupling between unsteady combustion processes and pressure waves in the combustion chamber [1–3]. Such instabilities enhance heat transfer to combustor walls, deteriorate combustion efficiency, increase pollutant emission, and, in extreme cases, can produce structural damages leading to the loss of control of the power plant or propulsion system.

Intensive experimental and theoretical work has been performed to understand the driving mechanisms of thermoacoustic instabilities, and to suppress these instabilities in laboratory-scale and full-scale combustors. While the global mechanism of thermoacoustic instabilities is known, identifying in real-time the responsible initial mechanism and its precursors remains a difficult task. This is partly due to the complexity of the involved mechanisms, for example the complicated interaction between flame chemistry, turbulent flow field and acoustic modes of a combustor, that results in an unsteady variation of the flame shape and the local reaction rates. During combustion instabilities three physical mechanisms interact in a highly nonlinear and unsteady manner, i.e., vortex motion (vorticity), heat release (entropy waves) and acoustic fluctuations, and the flame itself can be influenced by noise and acoustic waves up to a resonant interaction [1,2,4]. In this interaction, equivalence ratio fluctuations are mostly responsible for heat release fluctuations; typically, acoustic oscillations in the premixer section cause fluctuations in the fuel and/or air supply rates, thus producing a reactive mixture whose equivalence ratio varies periodically in time, and that, when convected to the flame front, produces heat release oscillations that drive the instability [2]. This justifies that apart from Lord Rayleigh postulate [5] or some different and new formulations [6,7] there are still no reliable criteria to predict self-excited combustion oscillations. Today's strategies for reducing combustion instabilities in practical gas turbines are mostly based on empirical methods.

The definition of precursors depends by the type of the (physically founded) warning signals employed to detect it. Commonly adopted precursor indexes are based on linear analysis, e.g., a pressure oscillation amplitude or a growth of the cross-correlation coefficient between pressure and heat release fluctuations [8]. In fact, pressure and heat release fluctuations, p' and H'_R, involved in the Rayleigh instability index, are governed by the Linearized Acoustic Energy Perturbation Balance Equations; furthermore, in the frequency domain any interdependencies are measured by the coherence function, based on cross spectral densities, or Fourier spectra of cross-correlations, that in turn suppose a linear interdependence between sampled quantities.

The simplest strategy to identify the precursor events of thermoacoustic instabilities is the threshold method, independently of the monitored quantities. This strategy is based on a relative measurement, that compares the current sample with the signal mean value, over a

---

[*] Corresponding author.
E-mail address: eugenio.giacomazzi@enea.it (E. Giacomazzi).

https://doi.org/10.1016/j.applthermaleng.2025.126927
Received 17 December 2024; Received in revised form 18 April 2025; Accepted 21 May 2025
Available online 30 June 2025
1359-4311/© 2025 The Author(s). Published by Elsevier Ltd. This is an open access article under the CC BY license (http://creativecommons.org/licenses/by/4.0/).

short time window prior to the event. An identification strategy based on a threshold method working on lower statistical moments (such as mean) provides good time response. It is important to note that since the acoustic pressure of a microphone has a zero mean value, the relative measure cannot be based on means but needs higher statistical moments, such as rms or kurtosis.

Often it is assumed that thermo-acoustic oscillations are periodic, with a dominant frequency and a fixed amplitude, thus exhibiting period limit cycle oscillations. However, the sole frequency domain signal analysis, adopted assuming a linear coupling before the thermo-acoustic limit cycle amplitude saturation, often appears no totally effective in combustion instability early detection. In fact, the power spectral analysis presumes the rough classification of combustion instabilities in two types, depending on their oscillation amplitude and frequency, as obtained from the power spectrum [9,10]: one is the “stable combustion”, represented by a limit cycle with small oscillation amplitude and no dominant characteristic frequencies; the other is the “unstable combustion”, represented by a limit cycle with a large oscillation amplitude and well-defined oscillation frequency. This classification may be insufficient for extracting and understanding the far more elaborate nonlinear behavior of combustors under unstable regimes.

Combustion noise manifests as deterministic chaos in stable operation conditions, and the transition to thermoacoustic instability occurs through a dynamical state recognized as intermittency [11–17]. Many research papers reported the existence of intermittent oscillations experimentally prior to limit cycle oscillations, i.e., bursts of periodic pressure oscillations appearing among aperiodic pressure fluctuations in an apparently random manner [18].

The power spectral analysis of the pressure and heat-release fluctuations has been widely used to characterize unstable combustion modes but may be insufficient for understanding and interpreting the physics underlying combustion instabilities because they are a complex phenomenon strongly affected by the inherent nonlinearity associated with chemical reactions, turbulent flow, and acoustic perturbations [10]. Recent experiments revealed that even simple thermo-acoustic systems exhibit nonlinear behavior, far more elaborate than period-1 limit cycle oscillations. Therefore, in addition to the conventional linear analysis, new approaches based on Nonlinear Dynamics will be required to characterize the unstable regimes in gas turbine combustors.

To overcome the linear stability analysis limits in characterizing unstable combustion regimes, the chaotic analysis was applied to pressure and radiant energy signals sampled in some industrial combustors [19–21]. Such an analysis is based on phases pseudo-space reconstruction, attractors, optimum time delay, the minimum embedding dimension, and the largest Lyapunov exponent. When the chaotic analysis is applied, a precursor can be revealed by a decrease in the chaos level measure [22]. This loss of chaos from combustion noise to combustion instability can be quantified to serve as a precursor to impending instability [23].

The nonlinear chaotic analysis of recurrence plot and its diagonal-wise quantification can be applied to calculate four indexes [11,18,19,22–25]: the τ-recurrence rate index, the τ-determinism index, the τ-average diagonal line length index, and the τ-entropy index. The recurrence properties of intermittent burst oscillations can be quantified using dynamical systems theory by tracking the distribution of the aperiodic segments in the measured signals. Several statistical measures may be constructed through such recurrence quantification that provide robust early warning signals to an impending instability [23]. The duration of such periodic bursts increases as the operating conditions approach combustion instability and finally the system transitions completely to self-sustained oscillations. Thus, the intermittency in pressure measurements, if quantified (e.g. using recurrence rate index), can act as a precursor of combustion instability.

In [12], an online method to detect combustion instability monitoring based on the translation error has been proposed: this method quantifies the degree of parallelism of trajectories in the phase space, and it can be used as a control variable to prevent combustion instability. The translation error is estimated for trajectories in the phase space constructed from short time series data of combustion-chamber pressure fluctuations. It is possible to monitor the combustion state to prevent combustion instabilities using the translation error quantity as a control variable.

The nonlinear interdependencies index between pressure and radiant energy fluctuations or between chemiluminescence and infrared energy fluctuations proved to be good indicators of thermoacoustic instabilities [20,21]. A precursor is identified by a nonlinear interdependencies index spike, even if this may happen together with a chaos rise.

Wavelet transform is a linear qualitative technique and it appears as a powerful tool to tackle the study of thermoacoustic instability when combined with chaotic analysis [26]. However, the definition of an instability detector based on chaotic time series analysis is still at an early stage. Furthermore, the high computational costs involved in the chaotic analysis makes it unsuitable for real time (online) monitoring and control applications, at least at present. The cross-correlation coefficient can be an optimal instability warning signal, due to its ability to early perceive self-sustained combustion oscillations and to reveal meaningful insights on unsteady combustor physics.

This article describes the results of real-time (online) monitoring of a turbulent lean-premixed flame by means of an optical system called Optical Diagnostics of Combustion (ODC), developed, validated, and patented in ENEA [9,20,27,28], and a pressure transducer. With the aim of looking for the best index for online identification of instability precursors, different indexes are suggested and compared.

2. Monitoring quantities and sensors

The development of diagnostic methods for monitoring combustion chambers is increasingly important due to the need for precise process descriptions. Precision is crucial for implementing efficient and reliable control and optimization methods, which are essential for allowing higher operating temperatures and creating more efficient and flexible combustion systems. Besides precision, simplicity in application as well as durability in operation are other important goals for any new sensor or measurement system.

Measuring conditions in gas turbine combustion chambers or high-pressure turbine sections is extremely challenging due to the harsh environment. Various sensors are used to monitor and ensure safe turbine operations, but these can fail under complex conditions. Parameters involved in thermoacoustic combustion instabilities, such as sound pressure and heat release rate, are key inputs for active feedback control. Sound pressure is easily measured by means of microphones or piezo pressure transducers, while photomultipliers and photodiodes can effectively measure the unsteady heat release rate of the flame and temperature fluctuations [29].

The main and direct outputs that an observer in front of a combustion process can capture are radiant energy (light emission) and noise (pressure waves): the radiant energy can be split into two contributions, the chemiluminescence emission in the UV–VIS range and the thermal emission in the NIR or IR range.

The most basic measurable quantity to monitor and characterize unstable combustion is dynamic pressure [1,12,16,17], by means of microphones and piezoelectric pressure transducers. These sensors are vital for monitoring high-speed pressure changes in gas turbine combustion chambers, where rapid temperature and pressure fluctuations impact efficiency and safety. It is observed that in enclosed systems, flames can be strongly influenced by the acoustic characteristics of the combustion chamber; therefore, the acoustic signature of a burner may change when it is installed in different combustion chambers (including the effects of dampers and cooling systems).

Both currently used microphones and piezoresistive sensors cannot resist high temperature; hence, they require cooling systems [30] or they have to be placed far from high temperature regions (this could be done since acoustic waves propagate throughout the entire combustion system), although this could lead to response delays and inaccuracies [31]. They also have limited lifespans and can fail.

To address these limitations, high-temperature pressure transducers have been developed. One example is an optical dynamic pressure sensor having a sapphire optical head that can be mounted close to the combustion zone [32–34]. This sensor uses interferometric techniques, relying on the movement of a diaphragm to measure pressure by detecting changes in an optical cavity. This setup, which includes a sapphire Fabry–Perot cavity, offers several advantages: resistance to electrical noise, long operational life at temperatures above 1000 °C, high sensitivity, and no need for external cooling.

Many features make radiant energy sensors appealing. Such devices are optical; hence, they are not intrusive. Exhibiting large bandwidth up to several kHz or even tens MHz, they are suitable for the study of flame dynamics and combustion instabilities or unsteady pulsed combustors as well as for the development of fast-response controllers.

The naturally occurring flame chemiluminescence in UV–VIS range is related to heat release and has proven to be extremely useful in characterizing unstable combustion in lean premixed combustion [29, 35–41]. Chemiluminescence is the radiative emission from electronically excited species. Its intensity is determined by the competition between the chemical reactions that produce such excited species and the collisional quenching reactions.

Chemiluminescence sensing requires collecting light at specific wavelength bands. In particular, emission from OH* (282.9 nm; 307–309 nm) and CH* (387 nm; 431.5 nm) radicals, occurring at distinctly different and relatively narrow-wavelength intervals, are good indicators of heat release rate [38] and flame front location [35]. It is observed that in combustion research the heat release is typically measured indirectly by sampling the radical emission spectrum in the flame or by using the Planar Laser-Induced Fluorescence technique with high-resolution spectrometers and complex data processing algorithms: however, such techniques cannot be applied in industrial real plants and online monitoring of combustion instabilities. Instead, single detectors, such as photomultipliers (PM), photodiodes (PD) or avalanche photodiodes (APD), coupled with bandpass filters at selected central wavelengths usually of the order of a few nm, are the most common option to detect radiant energy in industrial applications [27].

As a drawback, such sensors require optical access to the system and may be susceptible to changes in flame location as the stability of the system changes. At least an optical head is required, looking at the reacting volume, and connected through optical fibers to the sensors, located far from the harsh environment of the combustor. The sampled radiant energy is integrated over the specific wavelength range of each photodiode, and spatially filtered over the control volume seen by the optical probe (a conical region). It is observed that there can be four different regions in the monitored combustor volume, respectively associated to cold reactants, to a thin reacting region (flame front), to hot products and to the “surrounding space”: the contribution of each of these regions to the sampled radiant energy is discussed in [27]. The positioning of the optical head in the combustion chamber is essential to observe as much of the reacting region as possible, in particular the flame front where radicals are formed.

Some coupled techniques, i.e., adopting both pressure and heat release sampling, were tested in gas turbines. Alstom obtained transfer functions in a high-pressure combustion test facility (EV-type test burner) from a set of multiple Rayleigh Criterion Probes (RCPs) combining acoustical and optical sensors [42–44]: the crucial aspect of this modeling approach was to obtain a correct representation of the interaction between the acoustic field and the heat release.

In this article, an optical system called Optical Diagnostics of Combustion (ODC) [9,20,27,28] and a pressure transducer, are adopted to monitor combustion condition changes over time while varying operating conditions of an industrial burner.

3. The suggested experimental instability criteria

The classical Rayleigh’s criterion [7] states that when the pressure and heat-release fluctuations, p' and H'_R, are in phase, a system becomes unstable:

$$\int_V \int_0^\tau p' H'_R dt dV > 0 \tag{1}$$

When the magnitude of the phase between p' and H'_R is less than 90° they can be assumed in phase, and the instability is locally amplified. Conversely, when these fluctuations are out of phase (i.e., in the range $90° - 180°$), the instability is damped.

Rayleigh’s criterion is a necessary but not sufficient condition for instability to occur (loss mechanisms are neglected). Chu’s criterion [7] is more accurate:

$$\int_V \int_0^\tau T' H'_R dt dV > 0 \tag{2}$$

It requires temperature and heat release fluctuations, T' and H'_R, to be in phase for the instability to grow.

An extended version of the above criteria also exists [7], where the quantities in Eqs. (1) and (2) must be greater than the acoustic losses through the boundary of the control volume:

$$\oint_A \int_0^\tau p' u' dt dA > 0. \tag{3}$$

Once introduced classical instability criteria, it is worth looking for some measurable integral (in space) quantities linked to T' and H'_R, that can be correlated to pressure fluctuations p'. To this aim, it is observed that total radiation emitted by flames consists of two types of sources: the first one is chemiluminescence, while the second one is thermal emission that can be associated to the Planck function [27,45, 46].

Since the intensity of light emission (radiant energy) in the UV–VIS range (chemiluminescence) is proportional to the production rate of some molecules (e.g., CH*, OH*, C_2^*), chemiluminescence can be used as an indicator of reaction rates and heat release rate fluctuations, i.e., H'_R [38]. Some studies have shown that the chemiluminescence emitted spontaneously by a lean hydrocarbon flame is proportional to the heat release [1]: if the equivalence ratio is constant, this relationship is perfectly linear [47], while it normally follows a power law.

Besides, since the intensity of light emission in the IR range (thermal energy) grows non linearly with temperature , it can be used as an indicator of temperature fluctuations, i.e., T' [45,46].

With these observations and statements, it is possible to define three instability criteria, $T' - H'_R$ (mimicking the Chu’s criterion), $p' - H'_R$ (mimicking the Rayleigh’s criterion), and $p' - T'$: they can be evaluated instantaneously and in real-time by cross-correlating the three quantities, H'_R and T' being measured via radiant energy sensors, and p' via acoustic sensors.

In particular, the three thermoacoustic instability indices are calculated as the integral area subtended by the absolute value of the cross-correlation coefficients. Pearson’s cross-correlation coefficient measures linear correlation between two sets of data and then the similarity of two signals; its possible range is from −1 to +1. Then the three thermoacoustic instability indices are dimensionless numbers and their value can vary between 0 (no linear dependency between the variables) and 1. In the case of “stable combustion” with small oscillation amplitude and no dominant characteristic frequencies the two sampled signals will have a weak correlation and these indices will have a low value, e.g., less than 0.20. In the case of “unstable combustion” with a large oscillation amplitude and well-defined oscillation frequencies, the two sampled signals will have a strong correlation and these indices will have a high value, e.g., larger than 0.50.

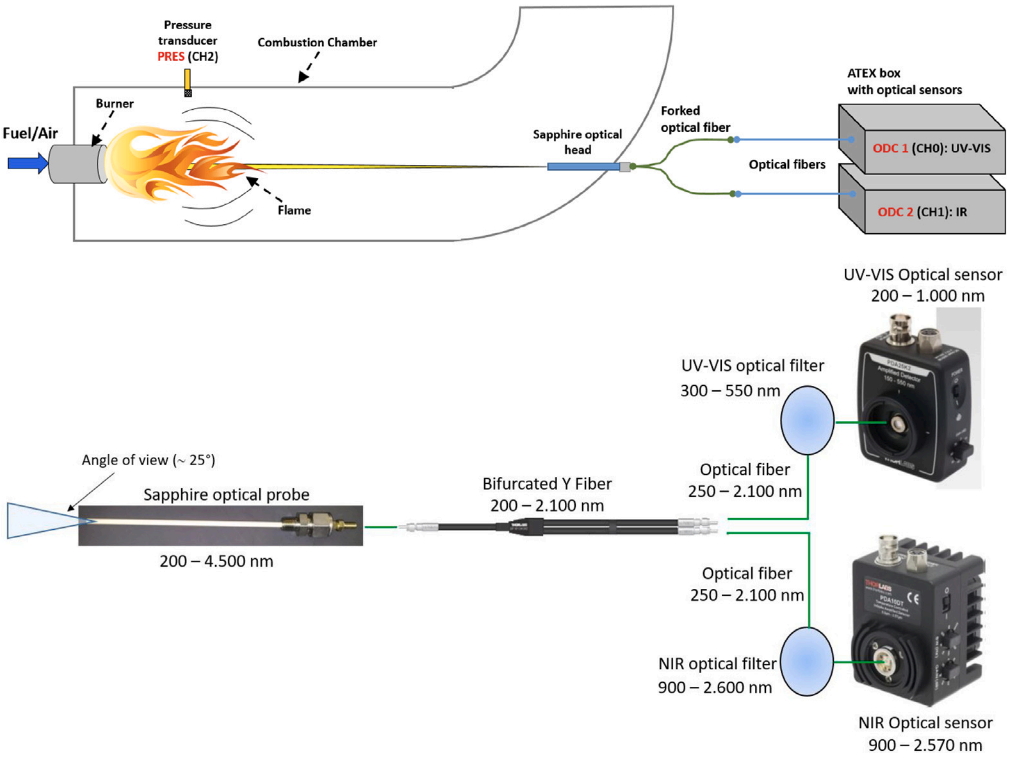

Fig. 1. Sketch of the experimental set-up.

4. Experimental set-up and combustor operation

The two integral radiant energy signals related to the UV–VIS and NIR ranges are sampled by means of the ODC system developed and patented at ENEA: the methodology lets to characterize in real time the dynamics of unstable conditions, chemical species, and temperature, and estimate the average flow speed [9,20,27,28].

The ODC system has an optical sapphire head with an angle of view of nearly 25°, that samples radiant energy from a wide reacting region to capture eventual growing of instability precursors in different parts of the flame. The sapphire has been selected mainly for its high temperature resistance, in addition to its chemical durability, thermal properties, and being an electrical insulator. The optical head is connected to two avalanche-photodiodes (APD) by means of a bifurcated optical fiber bundle (Fig. 1). The first APD works in the UV–VIS range (200–1000 nm, coupled to a pass-band optical filter limiting the actual range to 300–550 nm) linked to the heat release fluctuations, H'_R, and the second one in the NIR range (900–2570 nm, coupled to a high-pass optical filter in the range 900–2600 nm) linked to the temperature fluctuations, T'.

The dynamic pressure transducer adopted in the experimental campaign to measure the pressure fluctuations p' is a PCB 102M220, having a calibration sensitivity of 0.1443 V/bara (= 1.443 mV/kPa).

The optical and pressure signals are sampled in continuous mode at 40 kHz (DAQ sampling frequency), and a signal averaging between 2 samples is applied to reduce noise. In the analysis of the time evolution of the Power Spectral Density of the quantities, a time windows of 1 s is adopted with a consequent frequency resolution of 1 Hz.

The industrial burner investigated in this work has two modules: a central swirled premixed burner and a pilot coaxial burner [48]. It is operated at 60 kW_t, ambient pressure, and fed with a mixture of natural gas (94.6/0.5/4.2/0.6%vol. of $\mathrm{CH}_4/\mathrm{C}_3H_8/\mathrm{C}_2H_6/\mathrm{N}_2$) and air. The combustion and cooling air mass flow rates are constant during operation; the total fuel mass flow rate is also constant (nominal equivalence ratio ~ 0.56), split between the two modules.

The split percentage between the premixed and pilot burners is changed during operation as shown by the black curve in Fig. 2, and the flame switches from stable to unstable mode when increasing the premixed contribution. Three ramping up/down cycles are operated in $\sim$ 8000 s changing the fuel split percentage between the pilot and premixed modules of the burner, while keeping constant the energy provided to the system (fuel flow rate). The first ramp has a slow 40%–100% premix split ramp in $\sim$ 2000 s, followed by fast ramping down in $\sim$ 500 s. The second cycle has a ramp 0%–80% premix split in $\sim$ 700s, turns quickly to 60% for $\sim$ 1250 s, then to 0% very quickly. It is observed that after the second cycle an acquisition problem of the premix split signal occurred, resulting in a synchronization issue with the other signals. The third cycle has a ramp 0%–100% premix split in $\sim$ 1500 s (faster than in the first cycle), then turns back to 0% very quickly.

5. Combustion dynamics characterization

This section describes and analyzes the data acquired during the experimental campaign in which the burner operation was changed from non-premixed to premixed mode as described in the previous section: Fig. 2 reports the split percentage between the premixed and pilot burners, evidencing the three ramping up/down cycles. Changing the split percentage between the premixed and pilot burners, the combustion mode becomes unstable, in particular in the first and third cycles. Five time-windows (from A to E), each of 1 s, will be examined as representative of different operating conditions.

Fig. 2 also shows the time evolution of radiant energy and pressure raw signals. It is observed that while the radiant energy signals refer to the full quantities (i.e., average plus fluctuation), the pressure signal refers only to its fluctuation. It is observed that while looking at the radiant energy raw signals some conclusions on the dynamics of the system can be drawn, the pressure fluctuation raw signal does not offer such advantage.

The first ramp is visible in the ODC UV–VIS signal all over the time, but only at the peak unstable condition (100% split) in the NIR (likely

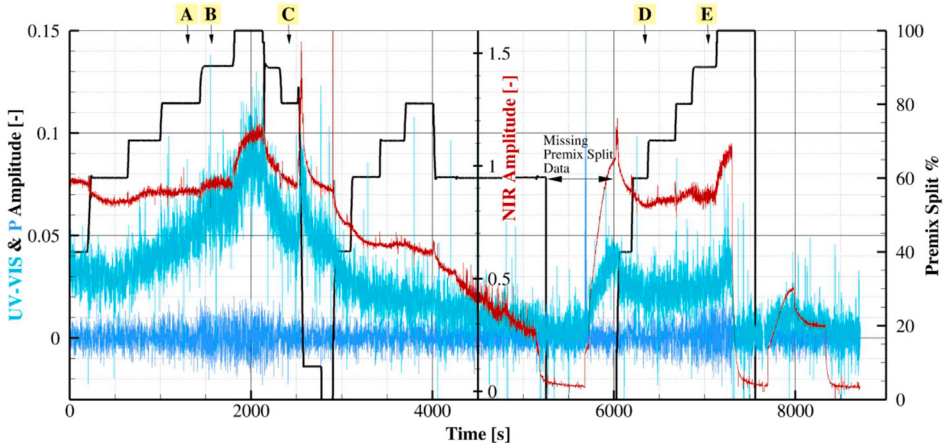

Fig. 2. Time–history of the ODC optical signals in the UV–VIS (heaven, left axis) and NIR (red, central axis) ranges, and of the pressure fluctuation signal (blue, left axis). The premix fuel split percentage is also reported (black, right axis).

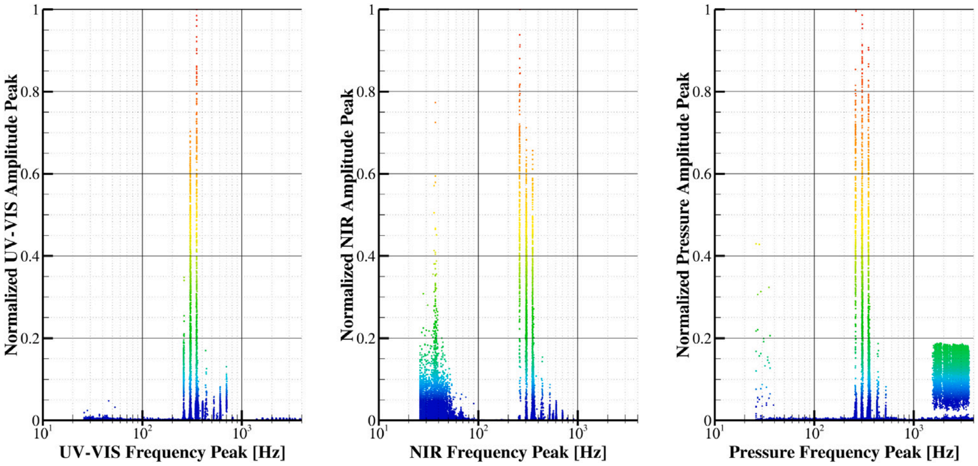

Fig. 3. Scatter plots of the first two frequency peaks and their amplitude (in both defined frequency ranges) for the ODC UV–VIS, NIR, and pressure signals (from left to right).

due to the inertia of the combustor walls); the fast ramping down is visible in both signals.

In the second cycle, both ODC radiant energy signals are monotonically decreasing, meaning that the combustor walls are slowly releasing the energy stored in the previous unstable pulsating state, while the energy provided through the fuel is constant and likely lower than the one released by the walls; no instabilities are detected by the radiant energy signals, likely prevented by the hotter condition of the system.

After the second cycle the temperature of the combustor walls lowered, as suggested by the decreasing trend of the NIR signal during the second cycle: hence, the system turns back to a state potentially able to become unstable again. In fact, the system exhibits an unstable condition revealed by both ODC radiant energy signals, especially by NIR.

5.1. Energy distribution in the frequency domain

The radiant energy and pressure raw data shown in Fig. 2 are now analyzed in detail in the frequency domain. In particular, the attention is focused on the first two frequency peaks in the (0–320) Hz and [320–4000] Hz ranges; this band separation was adopted since the acoustic resonance frequency of the experimental combustor facility is around 320 Hz.

The amplitudes and frequencies of the first two peaks experienced during the three cycles are shown in Fig. 3 for the three sampled signals. The tonal distribution of energy around 320 Hz is clearly visible in every signals. While the UV–VIS signal only marks the pulsation of the flame front, being related to heat release fluctuations, the NIR signal also reveals a lower frequency pulsation, around 40 Hz, that can be related to the large coherent turbulent scales in the combustor, marked by means of temperature fluctuations [27]: in fact, assuming the liner diameter $D = 116$ mm as the turbulent macroscale with a velocity fluctuation $u' \sim 5$ m/s (10% of the inlet bulk velocity), the macroscale frequency is nearly 40 Hz. The pressure signal, besides the dominant tonal distribution around 320 Hz, also reveals a lower amplitude, high frequency and nearly steady (as shown later on) distribution of acoustic energy around 2000 Hz, likely due to small scale injectors. Such observations stress that the three considered quantities provide complementary information, and once integrated, a good view of the dynamics of the system.

Fig. 4 reports the time history of the first two frequency peaks in the (0–320) Hz and [320–4000] Hz ranges: both frequencies and their amplitudes are shown. Looking at the amplitude of the three signals, it is observed that the two unstable conditions (in the first and third cycles), previously supposed just looking at the radiant energy raw signals, are now clearly evidenced. Such instabilities exhibit strong acoustic emissions around the resonant frequency of the combustor facility; in fact, when the instabilities are fully established, the system exhibits a clear tonal behavior, i.e., the energy is concentrated at specific frequencies and not spread over a wide range of frequencies.

Just as an example, Fig. 5 reports the Power Spectral Density (PSD) of the ODC NIR radiant energy signal in the five temporal windows

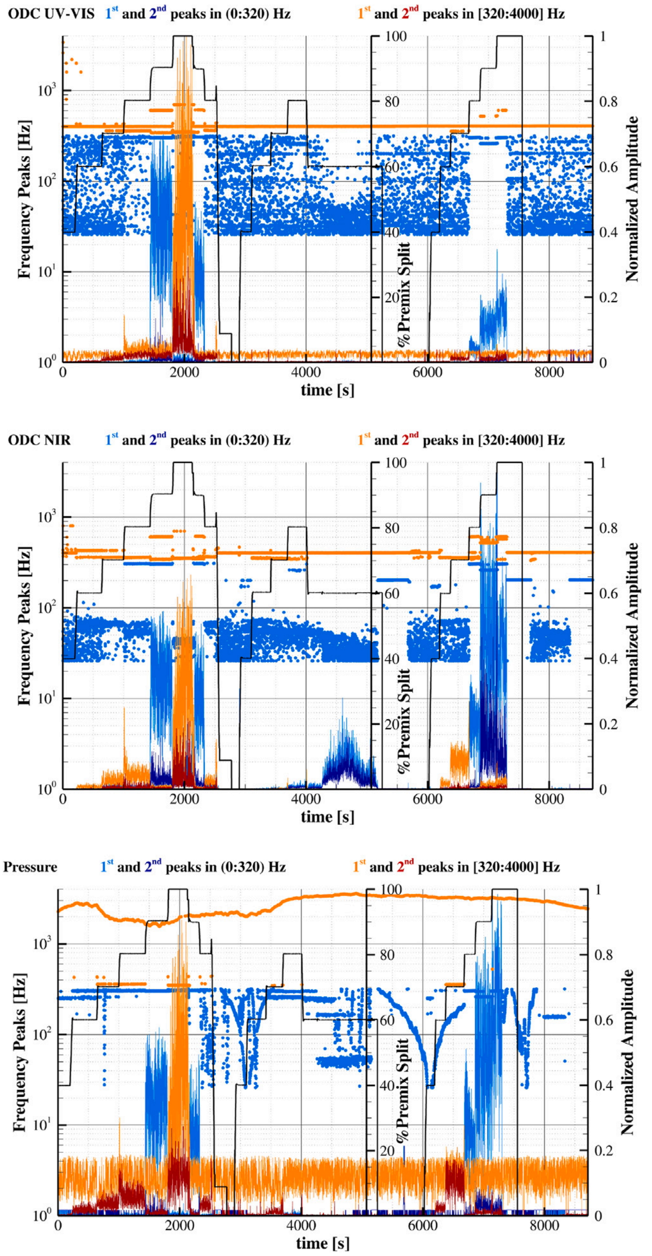

Fig. 4. Time–history of the first two frequency (dots) peaks and their amplitude (lines) for the ODC UV–VIS, NIR, and pressure signals in the frequency ranges 0–320 Hz and 320–4000 Hz. The premix fuel split percentage is also reported (black, right axis).

lasting 1 s (from A to E) marked in Fig. 2. It is observed that the spectra do not exhibit a clearly defined turbulence inertial range as in past more stable experiences [27], since the unstable resonant modes belong to this range.

6. Practical combustion instability indexes

With the goal of defining some practical instability indexes for the online characterization of the combustion stability system, different approaches are now investigated.

6.1. Cross-correlation indexes

The “instantaneous” cross-correlation indexes $T' - H'_R$, $p' - H'_R$ and $p' - T'$, shown in Fig. 6, are remarkably sensitive in all cases; the cross-correlation index between the ODC NIR optical signal and the pressure signal, i.e., $p' - T'$, performs better than the others, reaching values between 0.5 and 0.65. The indexes $T' - H'_R$ and $p' - H'_R$ look very similar: this could imply that T' and p' might be interchangeable, although having very different origins and interpretations, and different roles in triggering and amplifying thermo-acoustic instabilities; this requires further investigation. Besides, the lower performance could be justified by the low signal to noise ratio observed for the UV–VIS contribution, H'_R.

6.2. Auto- and cross-correlations

Fig. 7 shows the “instantaneous” auto-correlation and cross-correlation coefficients at condition E of Fig. 2. It is noted that in conditions of strong thermo-acoustic instability their shape tends to be rhomboidal, with considerable area coverage. This means that, if correlation indexes were defined as the integral area subtended by the cross-correlation coefficients, fully unstable systems would exhibit values tending to the dimensionless value of 1.

6.3. Signal’s power monitoring

Upon the previous observations, a different approach can be adopted. Fig. 8 reports the time–history of the integral of the “instantaneous” Power Spectral Density of the three analyzed signals. The integral of the PSD is here computed in the range $[1 - 2000]$ Hz containing most of the energy: this quantity is the average power or variance of the signal every 1 s. The trend of the pressure related quantity follows the premix split percentage cycles. The UV–VIS related quantity identifies only the well-established instabilities in cycles 1 and 3. The NIR one identifies both well-established instabilities and thermal changes of the system, but cannot discriminate the orientation of the transformation, i.e., if temperature is increasing or decreasing. Hence, besides cross-correlations, also this strategy could be promising.

To better identify the frequency range more affected by the instabilities, the integral of the PSD in the ranges [1:100] and [100–1000] Hz were calculated and reported in Fig. 9. The blue lines are related to the low frequency range, and hence to the large turbulent scales dynamics: it is observed that with this approach, the pressure signal provides information on such scales too. The red and green lines are related to the higher frequency range, and they better identify the combustion instability dynamics.

7. Challenges for implementation in industrial applications

The article described a novel approach for detecting combustion instabilities in industrial systems, applicable for online monitoring and integration into control systems. However, there are many challenges when dealing with industrial applications:

- the flame radiant energy diminishes when lowering the equivalence ratio (Dry Low Emission gas turbines operate with lean mixtures);
- the flame radiant energy diminishes when increasing the hydrogen content in the fuel mixtures (at present, there is a large interest in fuel-flexible gas turbines, i.e., able to stably operate with blends of natural gas and hydrogen, or ammonia and hydrogen);
- pressure affects the flame radiant energy (large gas turbines operate at nearly 25 bar, and micro-gas turbines at nearly 5 bar);
- the monitored combustor volume must be large enough to include the reacting region;
- the harsh environment of the combustor can affect the operability and lifetime of the optical head.

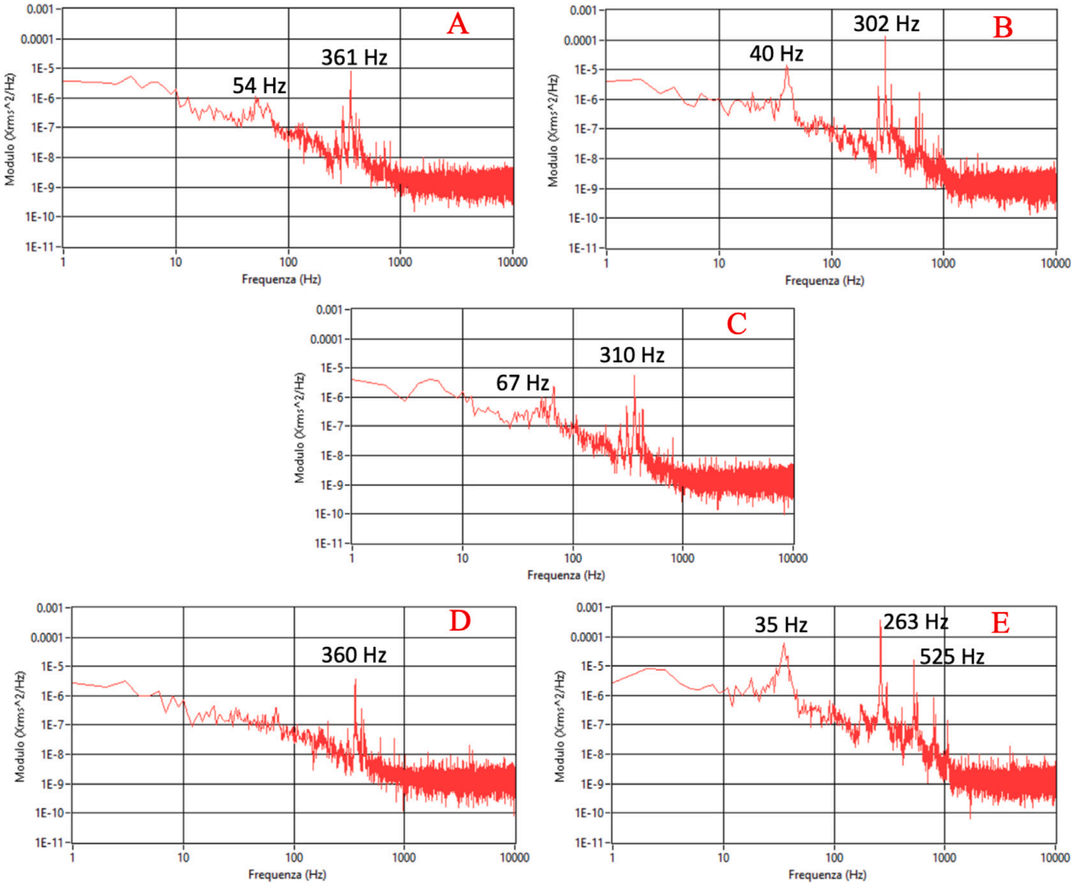

Fig. 5. Power Spectral Density of the ODC NIR radiant energy signal in the 1 s time-windows marked in the time–history diagram of Fig. 2, also reported here for convenience.

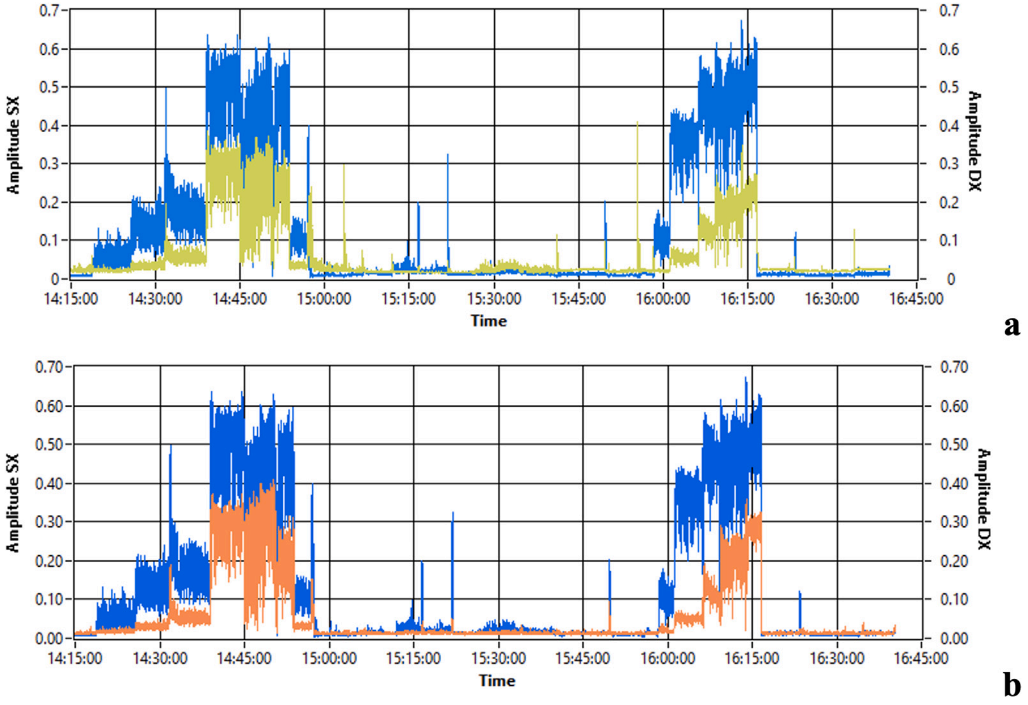

Fig. 6. Time–history of the cross-correlation indexes between the ODC signals in the UV–VIS and NIR ranges (light green), the ODC NIR and pressure signals (blue), and the ODC UV–VIS and the pressure signals (orange).

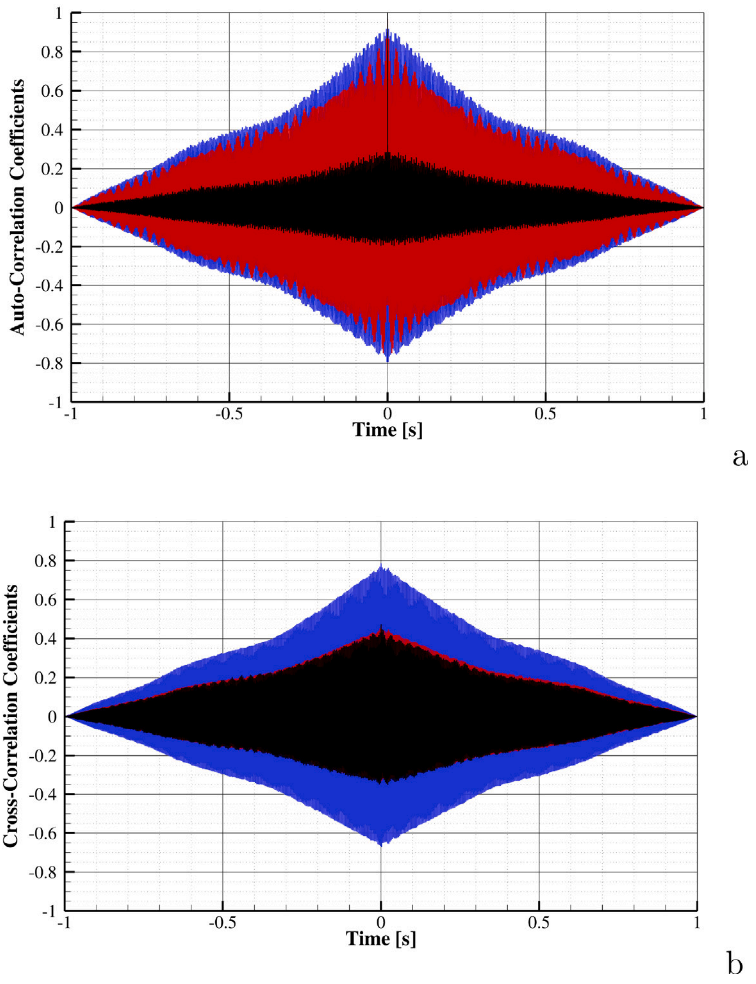

Fig. 7. Condition E of Fig. 2: (a) auto-correlation coefficients for ODC signals in the UV–VIS (black) and NIR (red) ranges, and for the pressure signal (blue); (b) cross-correlation coefficients between the ODC signals in the UV–VIS and NIR ranges (black), the ODC UV–VIS and the pressure signals (red), and the ODC NIR and pressure signals (blue).

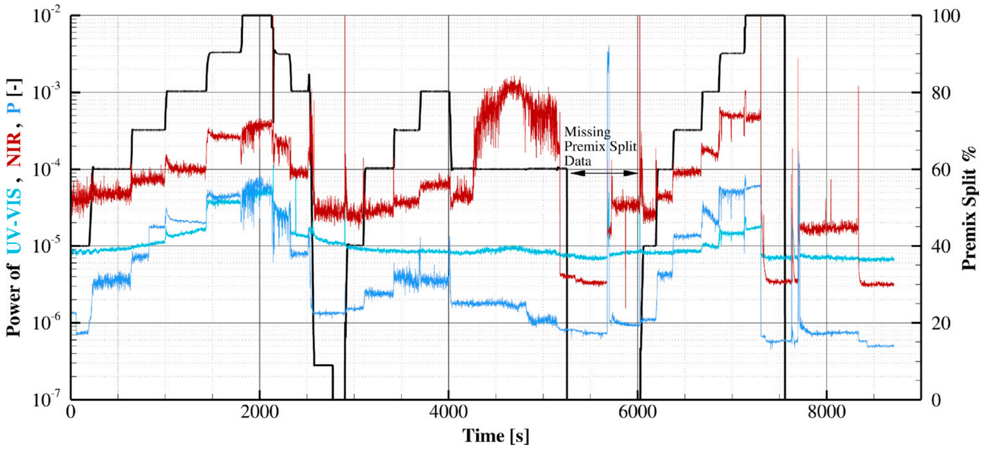

Fig. 8. Time–history of the integral of the Power Spectral Density spectrum of the three analyzed signals in the range [1–10000] Hz: UV–VIS (heaven), NIR (red), pressure (blue). The premix split curve is also reported (black).

Concerning the effect of the equivalence ratio, it is observed that for natural gas and air flames, the UV range contribution to the flame radiant energy (here linked to heat release fluctuations) reduces when reducing the equivalence ratio since chemiluminescence emissions of OH^*, CH^*, C_2^* and CO_2^* decrease [38,40,42,49–51].

The UV contribution also decreases when increasing the hydrogen content in the fuel [40,52]; in particular, the CH^*, C_2^* peaks of methane flames completely disappear in hydrocarbon-free flames, such as hydrogen [47] or syngas [53] flames.

Pressure largely affects the radiant transfer of energy [52]. Increasing pressure causes a broadening of the spectral lines, mainly due to molecular collisions, resulting in broader and more overlapping spectral lines than at lower pressures: the result is that the gas becomes "greyer" (opaque). In particular, the peaks of OH^*, CH^* and C_2^* decrease

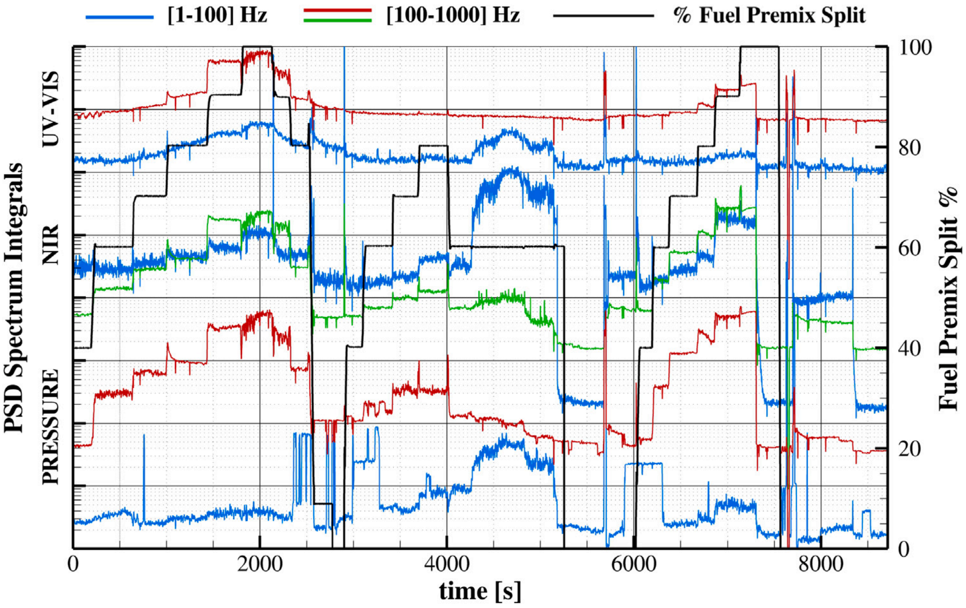

Fig. 9. Time–history of the integral of the Power Spectral Density spectrum of the three analyzed signals in the ranges [1–100] and [100–1000] Hz: UV–VIS, NIR, and pressure. The premix split curve is also reported (black).

with respect to the continuum background [54]; in fact, pressure increases the frequency of intermolecular collisions that becomes intense enough to de-excite the radicals (collisional quenching) [49,55–57]. The effect of pressure on the absolute intensities of OH^* and CH^* per unit of fuel mass flow rate has also been quantified and modeled as $p^{-0.86}$ [49] and $p^{-0.22}$ [50], respectively.

The positioning of the optical head in the combustion chamber is essential to observe as much of the reacting region as possible. To this aim, it is preferable to design an optical head with the widest possible viewing angle: a wide-angle sapphire optical head would be of help.

Concerning the industrial environment, the adoption of an optical head (the probe) and optical fibers let to locate the sensors far from the combustor harsh environment. This moves most of the problems on the design of the optical head, that requires suitable materials (as sapphire) to face high temperatures, and, depending on the location in the combustor, some specific fluxing solutions to avoid materials deposition (e.g., soot) and the consequent acquired signal attenuation.

8. Conclusions and future work

The growing of instabilities is a complex problem, where different factors like system thermal inertia, ramp rate from pilot mode to premixed mode, and geometric configuration, can play important roles.

An online practical method to monitor the dynamic state of combustion systems and to detect thermoacoustic instabilities, consisting in sampling flame radiant energy using a photodiode and employing cross-correlation indices, has been proposed: unlike what stated in [19], the linear analyses based on cross-correlation coefficients is capable of detecting combustion instabilities; furthermore, it is suitable for implementation in online control systems of industrial burners. The other approaches adopted in the article to analyze the sampled signals provide further support and could open promising ways for new instability indexes.

In particular, to justify the strategy of sampling radiant energy using photodiodes for an extended version of the classical Rayleigh's criterion and Chu's criterion, three simple, practical and experimental thermoacoustic instability indices were identified, $T' - H'_R$, $p' - H'_R$ and $p' - T'$, that are dimensionless numbers varying between 0 and 1. The high cross-correlation $p' - T'$ suggests the two quantities might be interchangeable, although being very different and triggering and amplifying thermo-acoustic instabilities in different ways. This point requires further investigation and could have important implications. In fact, this strategy, if confirmed, would have the potential to reduce monitoring hardware by substituting the flame detector with a robust optical sapphire head.

Future work will aim to enhance the optical signal sampled in the UV–VIS range by reducing the number of junctions between optical fibers and utilizing a more sensitive GaP (Gallium Phosphide) optical sensor operating in the 150–550 nm range. With these new features, the performance of the cross-correlation indices will be reassessed to determine whether combustion instabilities can be detected solely using the ODC system, focusing on monitoring the $T' - H'_R$ index.

Declaration of competing interest

The authors declare the following financial interests/personal relationships which may be considered as potential competing interests: ENEA reports financial support was provided by European Union (NextGeneraionEU) through the Italian Ministry of Environment and Energy Security. If there are other authors, they declare that they have no known competing financial interests or personal relationships that could have appeared to influence the work reported in this paper.

Acknowledgments

This study was performed within the Italian project "Research and Development of Technologies for Hydrogen Chain", POR-H2, WP2, LA2.2.5, funded by the European Union (NextGeneraionEU) through the Italian Ministry of Environment and Energy Security, under the National Recovery and Resilience Plan (PNRR, Mission 2, Component 2, Investment 3.5, project code I83C22001170006).
Special thanks to Nuovo Pignone Tecnologie Srl, a part of the Baker Hughes group, for generously granting access to their facility and providing the experimental data.

Data availability

The authors do not have permission to share data.

References

[1] T. Lieuwen, V. Yang, Combustion instabilities in gas turbine engines: operational experience, fundamental mechanisms, and modelling, Prog. Astronaut. Aeronaut. 210 (2005) 611–634.

[2] T. Lieuwen, V. McDonell, E. Petersen, D. Santavicca, Fuel flexibility influences on premixed combustor blowout, flashback, autoignition, and stability, J. Eng. Gas Turbines Power 130 (2008) 011506(1–10).

[3] E. Giulietti, Combustion Instabilities in Gas Turbine - A New Methodology for Combustion Monitoring, LAP LAMBERT Academic Publishing, 2015.

[4] Y. Huang, V. Yang, Dynamics and stability of lean-premixed swirl-stabilized combustion, Prog. Energy Combust. Sci. 35 (4) (2009) 293–364.

[5] J.W.S. Rayleigh Lord, The explanation of certain acoustic phenomena, R. Inst. Proc. Nat. Lond. 8 (1878) 536–542.

[6] B.T. Chu, On the energy transfer to small disturbances in fluid flow (part i), Acta Mech. 1 (1965) 215–234.

[7] F. Nicoud, T. Poinsot, Thermoacoustic instabilities: Should the Rayleigh criterion be extended to include entropy changes? Combust. Flames 142 (2005) 153–159.

[8] R. Bruschi, E. Giacomazzi, E. Giulietti, C. Stringola, M. Nobili, T. Pagliaroli, S. Giammartini, An optical technique for the identification and tracking of combustion instabilities, in: Proc. 7th Mediterranean Combustion Symposium the Combustion Institute, Cagliari (Italy), 11-15 September, 2011.

[9] R. Bruschi, E. Giacomazzi, C. Stringola, CasasantaV, F. Manfredi, M. Caruggi, Diagnostics of flow dynamics bringing to the onset of thermo-acoustic instabilities in gas-turbine combustors, in: 14th IFRF Members' Conference Noordwijkerhout, The Netherlands, 11-14 May, 2004.

[10] H. Gotoda, H. Nikimoto, T. Miyano, S. Tachibana, Dynamic properties of combustion instability in a lean premixed gas-turbine combustor, Chaos 21 (1) (2011).

[11] V. Nair, G. Thampi, R. Sujith, Intermittency route to thermoacoustic instability in turbulent combustors, J. Fluid Mech. 756 (2014) 470–487.

[12] H. Gotoda, Y. Shinoda, M. Kobayashi, Y. Okuno, S. Tachibana, Detection and control of combustion instability based on the concept of dynamical system theory, Phys. Rev. E 89 (2) (2014) 022910(1–8).

[13] M. Murugesan, R.I. Sujith, Combustion noise is scale-free: transition from scale-free to order at the onset of thermoacoustic instability, J. Fluid Mech. 772 (2015) 225–245.

[14] R. Sampath, S.R. Chakravarthy, Investigation of intermittent oscillations in a premixed dump combustor using time-resolved particle image velocimetry, Combust. Flame 172 (2016) 309–325.

[15] V.R. Unni, R.I. Sujith, Flame dynamics during intermittency in a turbulent combustor, Proc. Combust. Inst. 36 (3) (2017) 3791–3798.

[16] A. Kushwaha, K. Praveen, S.A. Pawar, R.I. Sujith, I. Chterev, I. Boxx, Dynamical characterization of thermoacoustic oscillations in a hydrogen-enriched partially premixed swirl-stabilized methane/air combustor, J. Eng. Gas Turbines Power 143 (12) (2021) 121022(1–11).

[17] A. Kushwaha, Thermoacoustic Oscillations in Hydrogen Enriched Turbulent Combustion (Ph.D. thesis), Department of Aerospace Engineering Indian Institute of Technology Madras, 2023.

[18] V. Nair, R. Sujith, A reduced-order model for the onset of combustion instability: physical mechanisms for intermittency and precursors, Proc. Combust. Inst. 35 (3) (2015) 3193–3200.

[19] T.Hernandez-Rivera.R. Pagliaroli, G. Troiani, A. Hernandez-Guerrero, Early detection of the combustion instabilities by quantifying diagonal-wise measurements of joint recurrence plots of pressure and radiant energy fluctuations, Phys. Fluids 34 (4) (2022).

[20] S. Chiocchini, T. Pagliaroli, R. Camussi, E. Giacomazzi, A mutual nearest neighbours based chaotic synchronization index to detect thermo-acoustic coupling in gas turbine combustion instabilities, GT2016-56222, Seoul, South Korea, June 13-16, 2016.

[21] S. Chiocchini, T. Pagliaroli, E. Giacomazzi, R. Camussi, Chaotic and linear statistics analysis in thermoacoustic instability detection, J. Propuls. Power 34 (1) (2017).

[22] V. Nair, G. Thampi, S. Karuppusamy, S. Gopalan, R. Sujith, Loss of chaos in combustion noise as a precursor of impending combustion instability, Int. J. Spray Combust. Dyn. 5 (4) (2013) 273–290.

[23] V. Nair, G. Thampi, R. Sujith, Engineering precursors to forewarn the onset of an impending combustion instability, in: Proc. ASME Turbo Expo 2014, in: Turbine Technical Conference and Exposition, American Society of Mechanical Engineers, 2014, pp. 1–7, GT2014-26020.

[24] R. Hernandez-Rivera, G. Troiani, T. Pagliaroli, A. Hernandez-Guerrero, Chaotic analysis of the thermoacoustic instabilities of a trapped vortex combustor, in: Proc. AIAA/CEAS Aeroacoustics Conference, 2018.

[25] R. Hernandez-Rivera, G. Troiani, T. Pagliaroli, A. Hernandez-Guerrero, Detection of the thermoacoustic combustion instabilities of a slot burner based on a diagonal-wise recurrence quantification, Phys. Fluids 31 (12) (2019).

[26] T. Pagliaroli, G. Troiani, Wavelet and recurrence analysis for lean blowout detection: An application to a trapped vortex combustor in thermoacoustic instability, Phys. Rev. Fluids 5 (7) (2020) 073201(1–16).

[27] E. Giacomazzi, G. Troiani, E. Giulietti, R. Bruschi, Effect of turbulence on flame radiative emission, Exp. Fluids 44 (4) (2008) 557–564.

[28] E. Giacomazzi, E. Giulietti, C. Stringola, S. Cassani, L. Pagliari, S. Chiocchini, Combustion monitoring in gas turbines and enhanced stability at very lean conditions, in: Proc. ASME Int. Gas Turbine Inst. ASME TURBO Expo: Power for Land, Sea, and Air, GT2014-25506, Dusseldorf, Germany, 2014.

[29] Y. Zhong, T. Zhang, Y. Zhang, T. Cheng, Flame temperature and heat release rate sensor for active combustion control, Measurement 202 (2022) 111762.

[30] M. Mersinligil, J.-F. Brouckaert, J. Desset, Unsteady pressure measurements with a fast response cooled probe in high temperature gas turbine environments, J. Eng. Gas Turbines Power 133 (8) (2011) 081603(1–9).

[31] R. Sun, L. Shi, X. Yang, Y. Wang, Q. Zhao, A coupling diagnosis method of sensors faults in gas turbine control system author links open overlay panel, Energy 205 (2020) 117999(1–12).

[32] A. Winterburn, R. Pechstedt, F. Maillaud, T. Roediger, O. Lammel, P. Griebel, Extension of an optical dynamic pressure sensor to measure temperature and absolute pressure in combustion applications, in: 6th International Conference of the Future of Gas Turbine Technology, 17-18 October 2012, Brussels, Belgium, 2012.

[33] F.C.P. Leach, M.H. Davy, D. Siskin, R. Pechstedt, D. Richardson, An optical method for measuring exhaust gas pressure from an internal combustion engine at high speed, Am. Inst. Phys. Rev. Sci. Instrum. 88 (2017) 125004.

[34] R.D. Pechstedt, A. Sposito, High-temperature fibre optical sensor, in: 26th International Conference on Optical Fiber Sensors, OSA, 2018.

[35] Y. Ikeda, J. Kojima, T. Nakajima, F. Akamatsu, M. Katsuki, Measurement of the local flame front structure of turbulent premixed flames by chemiluminescence, Proc. Combust. Inst. 28 (1) (2000) 343–350.

[36] J. Kojima, Y. Ikeda, T. Nakajima, Spatially resolved measurement of OH*, CH*, and C2* chemiluminescence in the reaction zone of laminar methane/gase premixed flames, Proceeding Combust. Inst. 28 (2000) 1757–1769.

[37] J. Kojima, Y. Ikeda, T. Nakajima, Measurement of the local flame front structure of turbulent premixed flames by local chemiluminescence, Reston, VA, in: Proceedings of the AIAA/ASME/SAE/ASEE, JPCE Conference, vol. 36, 2000, pp. 3394–3405.

[38] Y. Hardalupas, M. Orain, Local measurements of the time-dependent heat release rate and equivalence ratio using chemiluminescent emission from a flame, Combust. Flame 139 (3) (2004) 188–207.

[39] J.-L. Beduneau, Y. Ikeda, Application of laser ignition on laminar flame front investigation, Exp. Fluids 36 (2004) 108–113.

[40] J. Ballester, T. García-Armingol, Diagnostic techniques for the monitoring and control of practical flames, Prog. Energy Combust. Sci. 36 (4) (2010) 375–411.

[41] C. Ruan, F. Chen, W. Cai, Y. Qian, L. Yu, X. Lu, Principles of non-intrusive diagnostic techniques and their applications for fundamental studies of combustion instabilities in gas turbine combustors: A brief review, Aerosp. Sci. Technol. 84 (2019) 585–603.

[42] B. Schuermans, F. Guethe, D. Pennell, D. Guyot, C.O. Paschereit, Thermoacoustic modeling of a gas turbine using transfer functions measured under full engine pressure, J. Eng. Gas Turbines Power 132 (11) (2010) 111503(1–9).

[43] G.E. Kraft, F. Giuliani, L. Pfefferkorn, N. Paulitsch, L. Andracher, Heat resistant probe combining optic and acoustic sensors for advanced combustion monitoring including detection of flame instabilities, in: The American Society of Mechanical Engineers (ASME), Turbo Expo: Power for Land, Sea and Air, 2017, Paper No: GT2017-63626.

[44] L. Andracher, F. Giuliani, N. Paulitsch, V. Moosbrugger, Progress on combined optic-acoustic monitoring of combustion in a gas turbine, in: The American Society of Mechanical Engineers (ASME), Turbo Expo: Power for Land, Sea and Air, 2021, Paper No: GT2020-1600.

[45] M. Planck, The Theory of Heat Radiation, second ed., New York, 1959.

[46] A.G. Gaydon, H.G. Wolfhard, Flames: Their Structure, Radiation, and Temperature, fourth ed., Chapman and Hall, London, 1978.

[47] V. Nori, J.M. Seitzman, Chemiluminescence measurements and modeling in syngas, methane and jet-a fueled combustors, in: Proc. 45th AIAA Aerospace Sciences Meeting and Exhibit, AIAA-2007-0466, 2007.

[48] A. Asti, F. Gamberi, G.Del. Vscovo, R. Carta, N. Giannini, M. Ignesti, C. Orazi, N. Pieroni, Heavy duty gas turbina performance and endurance testing: the NovaLT 16 experience, in: Proc. ASME Int. Gas Turbine Inst. ASME TURBO Expo: Power for Land, Sea, and Air, GT2018-76350, Lillestrom (Oslo), Norway, June 11-15, 2018.

[49] B. Higgins, M.Q. McQuay, F. Lacas, J.C. Rolon, N. Darabiha, S. Candel, Systematic measurements of OH chemiluminescence for fuel-lean, high-pressure, premixed, laminar flames, Fuel 80 (1) (2001) 67–74.

[50] B. Higgins, M.Q. McQuay, F. Lacas, S. Candel, An experimental study of the effect of pressure and strain rate on CH chemiluminescence of premixed fuel-lean methane/air flames, Fuel 80 (11) (2001) 1583–1591.

[51] A. Cipriano, S. Gasperetti, G. Mariotti, E. Paganini, Analysis of the spectral properties of premixed and diffusion natural gas flames at different scales, in: Proc. European Combustion Meeting, ENEL Produzione - Ricerca Pisa, Italia, 2003.

[52] E. Giacomazzi, G. Troiani, A.Di. Nardo, G. Calchetti, D. Cecere, G. Messina, S. Carpenella, Hydrogen combustion: Features and barriers to its exploitation in the energy transition, Energies 16 (20) (2023) 7174(1–29).

[53] R.W. Schefer, W.D. Kulatilaka, B.D. Patterson, Visible emission of hydrogen flames, Combust. Flame 156 (6) (2009) 1237–1241.

[54] N. Docquier, F. Lacas, S. Candel, Closed-loop equivalence ratio control of premixed combustors using spectrally resolved chemiluminescence measurements, Proc. Combust. Inst. 29 (1) (2002) 139–145.

[55] J.R. Howell, R. Siegel, M.P. Menguc, Thermal Radiation Heat Transfer, fifth ed., CRC Press, Taylor and Francis Group, 2010.

[56] M.F. Modest, D.C. Haworth, Radiative Heat Transfer in Turbulent Combustion Systems, in: Springer Briefs in Applied Sciences and Technology, Springer, 2016, p. 138.

[57] C. Caliot, G. Flamant, Pressurized carbon dioxide as heat transfer fluid: Influence of radiation on turbulent flow characteristics in pipe, AIMS Energy 3 (2) (2014) 172–182.